

# Flexural Behaviour of Reinforced Slab Panel System with Embedded Cold-formed Steel Frames as Reinforcement

Cher Siang Tan<sup>a</sup>, Yee Ling Lee<sup>a\*</sup>, Shahrin Mohammad<sup>a</sup>, Siong Kang Lim<sup>b</sup>, Yeong Huei Lee<sup>a</sup>, Jee Hock Lim<sup>b</sup>

<sup>a</sup>Faculty of Civil Engineering, Universiti Teknologi Malaysia, 81310 UTM Johor Bahru, Johor, Malaysia

<sup>b</sup>Faculty of Engineering & Science, Universiti Tunku Abdul Rahman, Kuala Lumpur, Malaysia

\*Corresponding author: yllee3@live.utm.my

## Article history

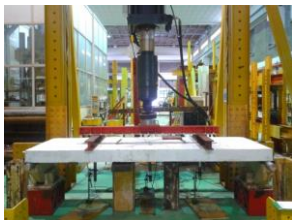
Received: 10 November 2014

Received in revised form:

23 January 2015

Accepted: 12 April 2015

## Graphical abstract



## Abstract

This paper presents the experimental investigation on flexural characteristic of slab panels with embedded cold-formed steel frame as reinforcement. Perforated cold-formed steel channel sections are formed into steel frames as replacement to the conventional reinforcement bars inside precast concrete slab panels. A series of six experimental specimens for precast slab panels were tested. The specimens with 3 configurations namely control sample (CS) with conventional reinforcement bars, single horizontal C-channel section (SH) and double horizontal C-channel sections (DH) formed into rectangular hollow section. Results show that the tested slab specimens failed at the flexural crack at mid-span, under loading point and shear at the support. Tearing of shear connector in the cold-formed steel section was found to be the main factor for the structural failure. SH specimens achieved the highest ultimate load capacity, with average value of 138.5 kN, followed by DH specimens, 116.5 kN, and the control samples, 59.0 kN. The results showed that the proposed reinforced slab panel with embedded cold-formed steel frame was more effective compared to conventional reinforced slab.

*Keywords:* Flexural resistance; slab panel; cold-formed steel; perforated; precast; channel section

© 2015 Penerbit UTM Press. All rights reserved.

## 1.0 INTRODUCTION

The conventional methods of building construction in Malaysia are reinforced concrete structures, timber structures, precast and prefabricated concrete, load bearing masonry etc. Traditionally for reinforced concrete, steel reinforcement bars, reinforcement grids, plates or fibers are added into the concrete in order to strengthen the concrete against tensile stress. Relatively low strength-to-self-weight ratio of reinforced concrete limits its design for large and long span members. Innovative concepts such as pre-stressed concrete and composite structure system are made available in Malaysia construction industry to overcome the limitation of reinforced concrete design.<sup>1</sup> A composite structure consists of two or more materials placed together in a structural element in such way that each material is used to its advantage and results in the best solution for the combination. Generally, composite structure system consists of concrete and steel, where concrete is utilized in compression zone, while steel are good in carrying tension forces.

For several decades, the application of composite structural members was largely used in bridge engineering<sup>2</sup> and building construction.<sup>3</sup> Composite slab system can be concrete slab act compositely with steel decking or conventional reinforced slab built on steel girders with shear studs, which latter generally referred as composite beam. The design has been well established

and anchored in the codes of practice.<sup>4, 5</sup> The codes mostly employ composite slab system by incorporating hot-rolled sections with shear transfer between the slab and beam provided by welded headed shear studs, or composite slab system with concrete and profiled cold-formed steel sheeting. Moreover, usually reinforcement bar that embedded in the concrete structures has problem on suffering early age degradation as corrosion of reinforcement steel is one of the factors of affecting it.<sup>6</sup> Researchers and engineers had continuously in doing the study on cost-effective means to prevent corrosion problem of reinforcing steel for the duration of concrete structure's design life.<sup>7</sup> So, in this study, cold-formed steel section was used as reinforcement as cold-formed steel is galvanized and protected from corrosion.<sup>8</sup>

Cold-formed steel (CFS) also known as light gauge steel had been used to build nearly 500,000 homes in USA over the past decade.<sup>9</sup> The typical thickness of cold-formed steel section is 0.9 to 3.2mm and.<sup>8</sup> Cold-formed steel section has the higher strength-to-weight ratio as compared to hot-rolled steel. They are formed at room temperature with the methods of cold-roll forming, press brake operation or bending brake operation.<sup>10</sup>

The application of cold-formed steel joists in composite floor system has gained its popularity in small commercial and residential construction in recent years.<sup>11</sup> The use of this type of composite slab system has been established in North America

with detailed design guidelines available in National Association of Home Builders of United States.<sup>11</sup> Critical element in the design of composite system is the shear connection. Shear connection enhances the strength capacity and rigidity of the composite slab. Contrasting with hot-rolled steel, cold-formed steel is relatively thin, where welding of the shear stud to the cold-formed steel sections might not be appropriate.<sup>12</sup> Other types of shear connectors in the market for cold-formed steel are available but at higher cost. One economical solution is by drilling holes on the cold-formed steel joist, making it perforated, so as to increase

the frictional force between concrete and cold-formed steel. However to achieve composite action, the perforated cold-formed steel joists must be fully embedded into concrete. There are very limited references in current codes of practice to the special problems involving composite slab system with embedded cold-formed steel sections. This study aims to determine the flexural behavior of prefabricated slab panels with perforated cold-formed steel channel sections embedded in concrete, through experimental investigation.

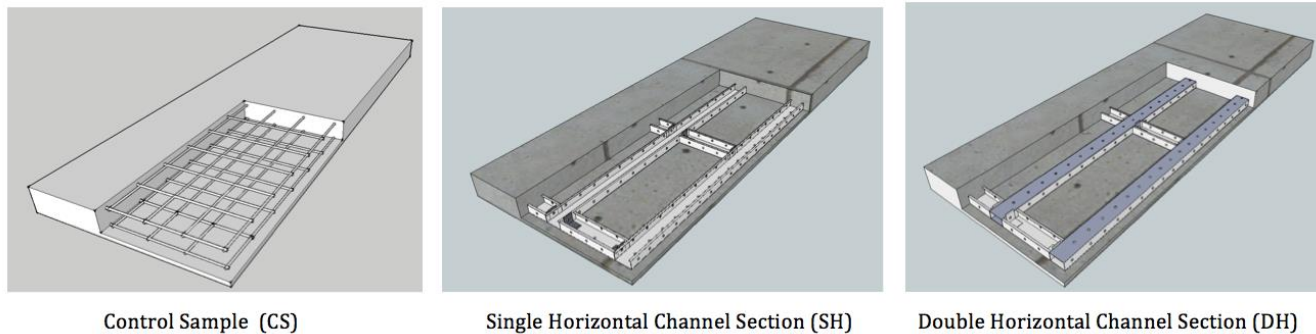


Figure 1 The cross sectional view of the three types of slab reinforcement configuration

## 2.0 EXPERIMENTAL PROGRAMME

In this study, combination of two different materials, which is normal weight concrete and cold-formed steel C-channel section are placed together to form a slab system. The cold-formed steel channel sections are perforated and formed into frame systems to replace reinforcement bar inside conventional concrete slab. Two types of reinforcement configurations using cold-formed steel frames are studied. Referring to the Figure 1, the first type of the slab configuration was three single cold-formed C-channel section placed horizontally as a built up steel frame (named as SH) whereas the second type of configurations was three double cold-formed C-channel section placed together as a rectangular hollow section and placed horizontally as a built up steel frame (named as DH). Control samples (CS) with conventional BRC steel reinforcement bar are prepared as well for comparison purpose.

Six full-scale slab specimens were tested in the experimental investigation, where two specimens were prepared for each type of CS, SH and DH slab panel configuration, as shown in Figure 1. Perforated cold-formed steel channel-sections (C-sections) were built up into steel frame and fully embedded into the concrete for SH and DH configuration. 12.5 mm diameter circular holes were drilled at an even spacing along the length of the flange and web of the cold-formed C-section to increase the efficiency of the interlocking between concrete and the smooth surface of CFS. The holes were spaced 100mm between two drilled holes. Bolts size with 12 mm diameter Grade 8.8 with two washers acts as the fastener were used to connecting the cold-formed steel (CFS) into a frame system.

### 2.1 Full-scale Tests

The six full-scale specimens, namely as CS-01, CS-02, SH-01, SH-02, DH-01 and DH-02, were tested to investigate the flexural resistance of the proposed slab system under pure bending. For specimens SH and DH, the CFS frame was fully replaced the

conventional reinforcement bar and embedded into the concrete slab. The dimension and location of CFS frame embedded in the concrete were 2.9 m length, 1 m width and 100 mm depth with positioned 25 mm from the bottom of concrete slab as referred to the previous study<sup>13</sup>. The dimension of CFS used for all specimens were channel sections with steel grade S450 and dimension of 100 mm web, 50 mm flange, 12 mm lips and 1.55 mm thickness. In each specimen, C-sections were held secure by intermediate C-sections with same CFS material and connected using brackets and M12 Grade 8.8 bolts with two washers. This subsequently formed a CFS frame. The CFS frame was placed in the middle of the formwork with 25 mm spacing for concrete cover. Reinforcements for control sample (CS) are grade S410 round steel bar with diameter of 10 mm and welded into square wire mesh of 100 mm distance, which generally named as BRC-A10.

The dimension of slabs was 3000 mm length, 1090 mm width and 150 mm thickness. Ready mix concrete that designed to achieve design strength of 35 MPa in 28 days is used. The slabs were casted with the ready mix concrete in wooden formwork, and cured for at least 7 days before commencing for flexural test. During the flexural test for each slab specimen, material testing on compressive strength and flexural strength for the concrete were carried out together. The details of each full-scale slab specimen are summarized in Table 1.

The typical slab test setup is as shown in Figure 2. A roller placed at each end and acted as simply supports. The test setup was according to the reference from the Eurocode 4.<sup>4</sup> Point load was applied at the fourth points of specimens through a spreader beam loaded at midpoint, thus generating a constant moment region at the centre span of the specimen. Hydraulic ram with capacity of 1200 kN was used to apply the load at the mid span of the spreader beam with the constant rate of 0.01 mm/s. The load from the ram was distributed to the two points on the test specimen.

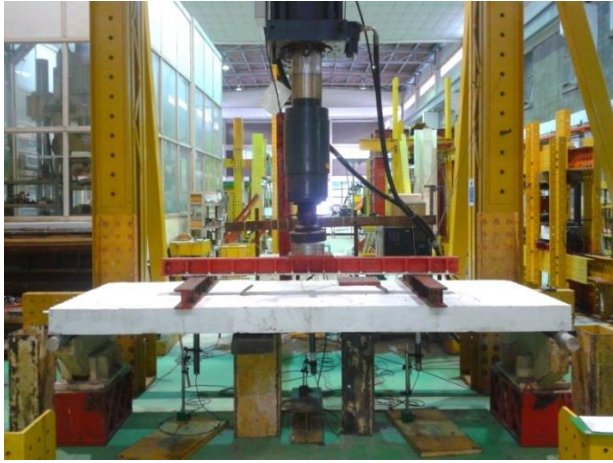
**Table 1** Details of full-scale precast slab specimens

Specimen	Reinforcement configuration <sup>1</sup>	Design strength of steel <sup>2</sup> , $f_s$ (MPa)	Compressive stress of concrete, $f_c$ (MPa)	Flexural stress of concrete, $f_{ct}$ (MPa)
CS-01	BRCA10 – Round steel bar with diameter 10 mm and welded into square wire mesh of 100 mm distance	410	37.4	5.7
CS-02			37.7	5.4
SH-01	Single CFS – Single perforated CFS channel section laid horizontally	450	36.8	5.1
SH-02			38.7	6.7
DH-01	Double CFS – Two perforated CFS channel section formed into a boxed section and laid horizontally.		40.2	6.2
DH-02			30.8	4.2

Note:

1. Reinforcement configuration for CS, SH and DH are depicted in Figure 1.

2. The design strength of steel are provided by the manufacturers. Coupon test for CFS channel section reaches ultimate tensile strength of 509.73 MPa.

**Figure 2** Test setup for large-scale specimens

For each specimen, there are three displacement transducers (DT) installed under the slab specimens with two DT installed at the bottom of loading point and one DT at the mid-span of the slab. Two DT are placed under the loading point to ensure the loading from both the loading point was in equilibrium. The DT at the mid-span was to measure the vertical deflection from the slab bending.

Nominal load of around 10% of the slab's designed load was first applied to the specimen and then released. This is to ensure that the testing specimens were settling in the test rig and instrumentation are well placed.<sup>11</sup> The load was gradually applied to each specimen until its failure. Load and deflection readings were monitored and recorded using an electronic data acquisition system. Cracks on the concrete slab surface were mapped and labeled with the load at which they occurred. Failure was deemed to have occurred where the specimen showed significant deflection and failed to take further loading.

## 2.2 Material Testing

Concrete cubes of 100 × 100 × 100 mm and beams of 100 × 100 × 500 mm were prepared at the same time during the casting of the full-scale slabs. The cube and beam were also cured under the similar condition with the full-scale testing specimens. The compressive strength and the flexural strength were tested according to BS EN 12390-5 and BS EN 12390-3.<sup>14,15</sup> Each of the material tests were carried on the same day commenced the slab specimen testing. The compressive and flexural strength results are included in Table 1.

## 3.0 RESULTS AND DISCUSSION

The experimental results are presented in Table 2, which including the ultimate load, the deflection at mid-span of the slab at the ultimate load, stiffness at the elastic region, load at allowable deflection and the mode of failure. Limiting value for the vertical deflection was adopted as 1/250 of the span length, which equal to 12 mm deflection limit.<sup>16</sup>

In the beginning, all the specimens have the similar cracking pattern as the failure was started by transverse cracking at the middle of the span. The cracks then propagated towards to the loading points. When the cracks spread to the top surface, the slab began to gradually lose its stiffness and bended in excessive deflection. At the ultimate load, flexural cracks and fractures occurred at the slabs and they failed to take additional loading. Three types of failure modes were observed for the six specimens: i) flexural cracks at the mid-span, ii) flexural cracks under loading point, and iii) failure in shear at the support cum fracture under loading point, as shown in Table 2 and Figure 3. The load-deflection graphs for all tests are depicted in Figure 4.

Figure 3 shows the failure modes of each the slab specimens. For specimens CS-01, CS-02 and SH-02, the flexural cracks happened at the mid-span. Specimens DH-01 and DH-02 both failed in shear at the support and fractured under the loading point. As for SH-01, the specimen failed under the loading point. All the specimens have the same failure mode within their own configuration except for the SH specimen. The different failure modes between the two SH specimens might due to the unbalanced loading during testing. Besides that, for the cracking control, the CS specimens have more cracks at the constant moment region. The cracks were spaced closely as compare to the slab panel with CFS frame as reinforcement. Furthermore, the DH specimens show the less cracking at the constant moment region. This may due to the higher reinforcement ratio, as higher reinforcement ratio suffered less cracking.<sup>17</sup>

By referring to Table 2, SH specimens showed the highest ultimate load among all specimens, achieving average value of 138.5kN. They were followed by DH specimens with average ultimate load of 116.5 kN and CS specimens with average 59.0 kN. Figure 4 shows the load versus mid-span deflection curve for all the tested specimens. Slab system with embedded CFS exhibited similar graph behaviour with the control sample, which is conventional slab system. Referring to previous study<sup>11</sup> the allowable deflection was fall at the elastic region. Nevertheless, in this study, the allowable deflection for all the specimens is falls in the plastic region. The load at allowable deflection is ranged from 44.9% to 69.9% of the ultimate load for all the tested specimens.

Table 2 Summary of test result

Specimen	Ultimate load, $P_u$ (kN)	Maximum mid-span deflection, $\delta_s$ (mm)	Stiffness (kN/mm)	Load at allowable deflection, $P_s$ (kN)	Failure mode
CS-01	54.5	39.24	19.83	32.5	Flexural cracks at the mid span
CS-02	63.5	38.92	14.17	33.0	Flexural cracks at the mid span
SH-01	138.0	52.02	17.51	62.0	Flexural cracks under loading point
SH-02	139.0	57.03	16.80	63.0	Flexural cracks at the mid span
DH-01	114.5	41.02	28.70	80.0	Failure in shear at the support cum fracture under loading point.
DH-02	118.5	41.02	29.30	68.0	Failure in shear at the support cum fracture under loading point.

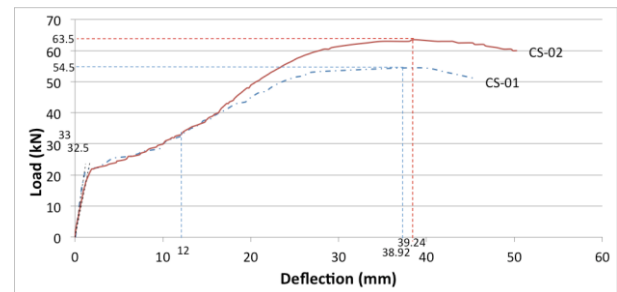


Figure 3 Failure modes for all specimens

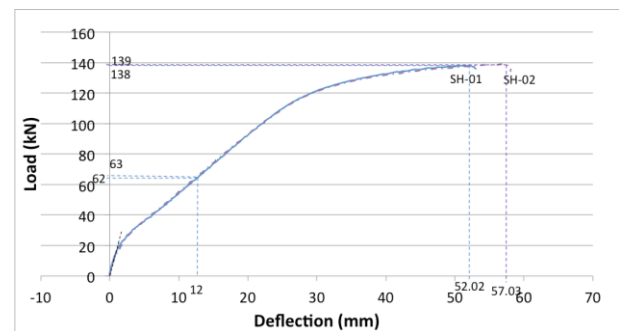
The load-deflection curve for specimen CS, as shown in Figure 4(a), the curve were linear up to 21.0 kN for CS-01 and 21.5 kN for CS-02, which is around 39% and 34% of the ultimate load respectively. The first noticeable transverse crack was observed at 22 kN and 23 kN respectively for the two CS slabs at the middle of the span. The specimens attained the ultimate load at 54.5 kN for CS-01 and 63.5 kN for CS-02. The rebar at the tension zone had fully yielded during the stage of ultimate load. From Figure 4(a), it also can be seen that the curve is not very smooth after achieved the elastic limit. This is due to the cracking in the specimen makes it achieved its serviceability and the load was mostly cater by the rebar in the tension zone. Figure 3(a) and Figure 3(b) shows the deflected shape of the specimen for CS-01 and CS-02.

For SH slabs, the load-deflection curve for specimen SH, as shown in Figure 4(b), the curves were linear up to 19.5 kN for SH-01 and 20.5 kN for SH-02, which is around 14.1% and 14.7% of the ultimate load respectively. The first noticeable transverse crack was observed at 19 kN for SH-01 and 17.5 kN for SH-02. The specimens obtained, on an average, 134.7% higher ultimate load than CS specimens, which is 138 kN for SH-01 and 139 kN for SH-02. Both the specimen has merely 0.7% of different at the ultimate load. SH specimens also obtained the highest average ultimate load among the three configurations. Although both the SH specimens failed at different point but both the SH slabs, with the CFS embedded inside the concrete, failed with the tearing of the drilled-hole

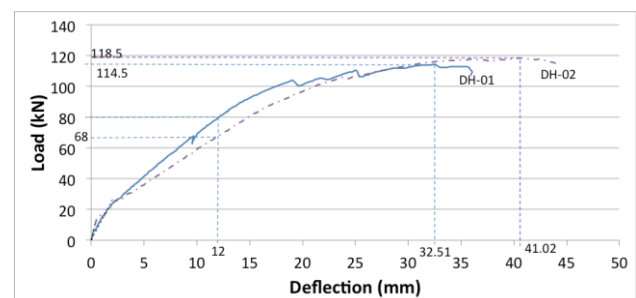
shear connector on the CFS surface. The tearing of shear connector is shown in Figure 5.



(a) CS



(b) SH



(c) DH

Figure 4 Load-deflection curve for all specimens

The load-deflection curve behaviour remains consistent for the DH specimens, which DH specimens comprising built-up the frame by placing two CFS C-sections into rectangular hollow section and placed horizontally. The first noticeable transverse crack was observed at 19.5 kN for DH-01 and 10.5 kN for DH-02. DH showed the second highest ultimate load but highest stiffness and withstood the highest loading during the allowable deflection. The DH specimen was believed to have the highest load resistance as it has higher steel cross-sectional

area, which it had been calculated from the previous study.<sup>18</sup> Conversely, the weakness of the hollow rectangular sections had the effect that the concrete was not fully occupying inside the built-up hollow section. This hence provide poor contact between the CFS and concrete, as the surface area for friction was less, hence making the DH specimen show lower load capacity than the SH specimen. Besides that, from the previous study on cold-formed beam flexural test<sup>19</sup>, it was known that cold-formed steel sections are tends to buckle. In this study, the hollow section that embedded in the concrete was buckle at the failure point. This was believed due to the concrete is not fully infill in the hollow part, the weakness of hollowness of the hollow section so tends buckle inwards.<sup>13</sup>



Figure 5 Tearing of shear connector

Based on the results, it is observed that the difference of ultimate load between CS-01 and CS-02 is 14.2%; SH-01 and SH-02 is 0.7%, and DH-01 and DH-02 is 3.4%. Thus it can be deduced that the test data are satisfying, with difference less than 15%.

The experimental results were comparing with analytical calculation by using the stress block method. Table 3 shows the comparison between the experimental and predicted moment capacity. Based on Table 3, it can be noted that the analytical calculation shows more conservative results except for the DH specimens, which is averagely about 21 % less than the predicted moment capacity. As for SH specimens, the experimental results averagely gives 42.5 % more than the predicted moment capacity. In addition, CS shows the most closed predicted moment capacity to the experimental result, which is 1 % and 16 % different for CS-01 and CS-02 relatively.

Table 3 Comparison of experimental and predicted flexural capacity

Specimen	Ultimate load, $P_u$ (kN)	Moment capacity, $M_u$ (kNm)	Predicted Moment Capacity, $M_{Ed}$ (kNm)	$M_u/M_{Ed}$
CS-01	54.5	19.76	19.89	0.99
CS-02	63.5	23.02	19.89	1.16
SH-01	138.0	50.03	35.18	1.42
SH-02	139.0	50.39	35.18	1.43
DH-01	114.5	41.51	53.19	0.78
DH-02	118.5	42.96	53.19	0.81

#### 4.0 CONCLUSION

Flexural behaviour of six slabs specimens with two different CFS configurations and one type of conventional BRC steel reinforcement as control sample was investigated. From the experimental result, several conclusions can be drawn:

- All slab specimens reached their design strength and failed after exceeding the allowable deflection. The differences of ultimate load between two test samples of the same configuration are less than 15%.
- Most of the slabs specimen failed by excessive deflection and flexural cracks at the middle of the slabs except that specimens for DH, which failed with shear at the support and fracture under the loading point and SH-01, which is failed under loading point.
- Based on the experimental result, slabs with single horizontal (SH) configuration achieved the highest ultimate load of 138.5 kN, followed by double horizontal DH (116.5 kN) and control sample, CS (59.0 kN).
- Most of the theoretical prediction of flexural capacity shows more conservative calculation if compare to the experimental results except for the DH specimens.
- Generally, the results showed that proposed composite cold-formed steel channel-section embedded in concrete was verified as being effective compared to conventional reinforced concrete.

#### Acknowledgement

The reported works in this paper have been supported by the Universiti Teknologi Malaysia, UTM Research Management Centre (Grants Vot 03H76 and Vot 4F258) and Ministry of Education Malaysia (MOE). The authors also express sincere gratitude to technical staff from Laboratory of Structures and Materials, Faculty of Civil Engineering.

#### References

- W. H. Wan Badaruzzaman, M. M. Zain, A. M. Akhand, & E. Ahmed. 2003. Dry Boards as Load Bearing Element in the Profiled Steel Sheet Dry Board Floor Panel System-Structural Performance and Applications. *Construction and Building Materials*. 17: 289–297.
- AASHTO. 2005. *AASHTO LRFD Bridge Design Specification*. 3rd ed. Washington (DC): American Association of State Highway and Transportation Officials.
- C. E. Ekberg & R. M. Schuster. 1968. *Floor System with Composite From Reinforced Concrete Slabs*. New York: IABSE.
- BSI. 2004. *Eurocode 4: Design of Composite Steel and Concrete Structures-Part 1.1: General Rules and Rules for Building*. London: British Standard Institution.
- AISC. 1993. *Load and Resistance Factor Desing, Specification for Structural Steel in Buildings*. Chicago: American Institute of Steel Construction.
- M. Ismail, E. Hamzah, C. G. Goh, and I. Abd Rahman. 2010. Corrosion Performance of Dual-phase Steel Embedded in Concrete. *The Arabian Journal for Science and Engineerin*. 35(2 A): 81–90.
- A. S. Abdulrahman, M. Ismail, and M. S. Hussain. 2011. Corrosion Inhibitors for Steel Reinforcement in Concrete: A Review. *Scientific Research and Essays*. 6(20): 4152–4162.
- Y. H. Lee, C. S. Tan, S. Mohammad, M. Md Tahir, and P. N. Shek. 2014. Review on Cold-formed Steel Connections. *The Scientific World Journal*. 2014: ID 951216.
- A. J. Way, S. O. Popo-Ola, A. R. Biddle & R. M. Lawson. 2009. *Durability of Light Steel Framing in Residential Building*. 2nd Edition (P262). Berkshire: The Steel Construction Institute.
- W. W. Yu. 2000. *Cold-formed Steel Design*. New York: John Wiley and Sons, Inc.

- [11] B. S. Lakkavalli & Y. Liu. 2006. Experimental Study of Composite Cold-formed Steel C-section Floor Joists. *Journal of Constructional Steel Research*. 62: 995–1006.
- [12] A. Hanaor. 2000. Tests of Composite Beams with Cold-formed Sections. *Journal of Constructional Steel Research*. 54: 245–264.
- [13] Y. L. Lee, C. S. Tan, Y. H. Lee, S. Mohammad, & P. N. Shek. 2012. Flexural Behaviour of Composite Slab Panel with Cold-formed Steel Section. *Joint conference 8th Asia Pacific Structural Engineering and Construction Conference-1st International Conference on Civil Engineering Research (APSEC-ICCER 2012)*. 162–166.
- [14] BSI. 2009a. *BS EN 12390-5 Testing Hardened Concrete-Part 5: Flexural Strength of Test Specimens*. UK: British Standard Institution.
- [15] BSI. 2009b. *Testing Hardened Concrete Part 3-Compressive Strength of Test Specimens*. UK: British Standard Institution.
- [16] D. Dubina, V. Ungureanu & R. Landolfo. 2012. *Design of Cold-formed Steel Structures*. Brussels: European Convention for Constructional Steelwork.
- [17] X. Gu, X. Song, F. Lin, C. Li, and X. Jin. 2011. Cracking Behaviour of Cast in Situ Reinforced Concrete Slabs with Control Joints. *Construction and Building Materials*. 25: 1398–1406.
- [18] Y. L. Lee, C. S. Tan, Y. H. Lee, S. Mohammad, M. M. Tahir & P. N. Shek. 2013. Effective Steel Area of Fully Embedded Cold-formed Steel Frame in Composite Slab System Under Pure Bending. *Applied Mechanics and Materials*. 284–287: 1300–1304.
- [19] Y. H. Lee, Y. L. Lee & C. S. Tan. 2012b. Experimental Investigation on Cold-formed Steel Beams Under Pure Bending. *Jurnal Teknologi*. 58: 13–20.